

Five-channel fiber-based laser Doppler vibrometer for underwater acoustic field measurement

JIANHUA SHANG,^{1,2,3,*} YANG LIU,¹  JIATONG SUN,¹ DAE WOOK KIM,⁴ WEIBIAO CHEN,⁵ AND YAN HE⁵

¹School of Information Science and Technology, Donghua University, Shanghai 201620, China

²Shanghai Center for High Performance Fibers and Composites, Shanghai 201620, China

³Center for Civil Aviation Composites of Donghua University, Donghua University, Shanghai 201620, China

⁴College of Optical Sciences, University of Arizona, Tucson, Arizona 85721, USA

⁵Shanghai Institute of Optics and Fine Mechanics, Chinese Academy of Sciences, Shanghai 201800, China

*Corresponding author: jhshang@dhu.edu.cn

Received 25 September 2019; revised 4 December 2019; accepted 9 December 2019; posted 10 December 2019 (Doc. ID 378788); published 15 January 2020

In this paper, a 1550 nm five-channel all-fiber homodyne laser Doppler vibrometer with high sensitivity and good signal probing probability is presented. Under the anechoic tank, standing on an airborne platform above the water surface 3 m away, the calibration experiments of the designed system are conducted. The minimum detectable sound pressure level is up to 101.73 dB re 1 μ Pa at 10 kHz under the hydrostatic water surface condition, and the time distribution of the final outputs are consistent with that of the underwater sound transducer. For the hydrodynamic detection capability, with the help of a 1064 nm high-pulse-energy laser whose pulse energy is 6J, pulse duration is about 8 ns, and repetition rate is 1 Hz, the system performance is tested in Qiandao Lake. And the signal probing probability of the whole sensing system is up to 59.77%. © 2020 Optical Society of America

<https://doi.org/10.1364/AO.378788>

1. INTRODUCTION

Based on the principle of the optical coherent detection, a laser Doppler vibrometer (LDV) is capable of presenting the high-precision vibration features of the measured surface in a non-intrusive and non-contact way. Unlike the ceramic-based hydrophone which provides a voltage proportional to the integral of the pressure variation when physically immersed in the acoustic field, employing the LDV to measure the underwater acoustic field from an aerial platform can give scientists a great opportunity to realize the acoustic signal reception without any mechanical perturbation by its presence [1–3]. Hence, this system plays a unique role in the field of the underwater acoustic signal detection, in which the vibration on the surface of a body of water has a close and fundamental physical relationship with the characteristics of the corresponding underwater sound sources. With the help of the Doppler frequency shift of the transmitted laser light, the instantaneous vibration velocity of this air–water interface can be obtained *in situ*.

LDV-based underwater sound sources detection has been proposed for many years. Furthermore, some experiments verifying the sensing and communication feasibility have been conducted under the hydrostatic and hydrodynamic

water surface conditions [4]. For the research regarding the hydrostatic condition, the main objective is to improve the minimum detectable sound pressure level (SPL) of the LDV-based acousto-optic remote sensing system and try to achieve identical detection sensitivity as that of the hydrophone [5]. Without a high sensitivity, the water surface vibration induced by the underwater sound source cannot be distinguished, especially when the air–water surface is rough and continually moving. On the aspect of the hydrodynamic water condition, there is a physical limitation resulting from the reflection characteristic of the water surface and the limited receiver's field of view. The moving water surface full with ripples and wave leads to the returned laser light deviated from the receiving telescope seriously. And the question of signal dropout is fatal. Recently, some studies and novel methods have been proposed to improve the performances for the application in practical situations [6–11].

Based on our previous research, the detection performance not only depends on the background noise or signal-to-noise ratio (SNR) of the LDV-based sensing system. It is also affected by the surrounding around it. In terms of the vibration of the platform, the air turbulence, and the structure of the water different from that of the solid, the detection sensitivity consequently decreases. In addition, the laser Doppler shift of the

coherent laser radiation induced by the in-water sound field is modulated by the fluctuation of the water surface, which puts forward a direct requirement for a high sample rate of the data acquisition card (DAC) consequently. In addition, with a large-diameter telescope, the signal probing probability of the returned signal can be improved indeed. However, the background noise of LDV-based sensing system is worsened and the minimum detectable SPL is increased at the same time. The detection sensitivity and the signal probing probability are the two fundamental factors for sensing. Only eliminating the signal dropout without enough detection sensitivity, it has no value for the practical acousto-optic sensing.

There are commercial LDVs available, including the single-point LDV, the scanning LDV, and the multi-point LDV. In our case, the requirements of the acousto-optic sensing are specific and more demanding than normal industrial applications. As mentioned above, the minimum detectable SPL is the fundamental factor for detection. Furthermore, the vibration caused by the underwater sound is mixed with the movement of the water surface (up to the level of m/s), which means the high-speed data acquisition must be applied. Therefore, we developed a most reliable compact single LDV and improved its detection abilities in order to make its minimum detectable SPL and the dynamic range similar to those of the hydrophone. Additionally, for the problem of signal dropout, we tried to capture the returned optical signal by means of the galvanometer scanning system. It can eliminate the signal dropout in an anechoic tank to some extent. Unfortunately, it leads to the background noise increase and fails to follow the motion of the water surface in a real lake. Therefore, the normal scanning LDV is not effective enough to obtain a weak returned signal with a good probing probability in the lake test.

In this paper, based on a high-sensitivity and large-dynamic-range single LDV, we resort to a five-channel fiber-based LDV to improve the probing probability of the experiments conducted under Qiandao Lake in Zhejiang province of China. Meanwhile, with respect to each channel, the minimum detectable SPL at different frequency bands is calibrated in the anechoic tank with the standard reference hydrophone. The rest of the paper is organized as follows: Section 2 introduces a review of the completed investigative measurements, including the description of the five-channel fiber-based LDV. Following, Section 3 presents the calibration test results from the anechoic tank experiment, along with the basic principle of conversion relationship for sound pressure level between the LDV and the hydrophone. And in Section 4, for the random air-water interface condition under Qiandao Lake, with five-channel LDV, the analysis and discussion of the experimental results are described. Finally, the conclusion and future research are provided briefly.

2. PRINCIPLES AND EXPERIMENTAL SETUP

With the help of the cost-effective telecom fiber optical components operating at eye-safe wavelength range, the five-channel LDV system can be compact and much more convenient to set up and optically adjust. Furthermore, the laser operating at the telecom band with long coherence length or narrow spectral linewidth, stealthy wavelength, lower relative intensity noise, and low phase noise offers a good choice to develop a

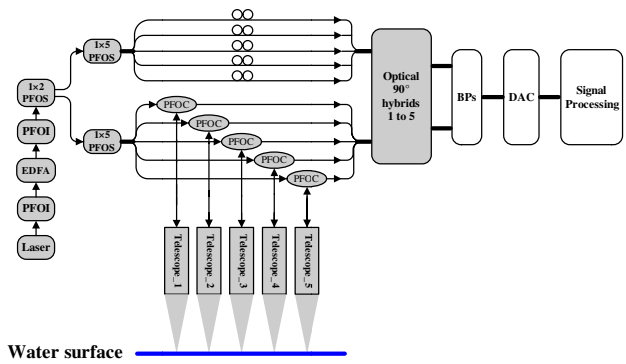


Fig. 1. Schematic layout of the five-channel LDV-based acousto-optic sensing system.

high-performance LDV. The schematic of the five-channel fiber-based LDV employing the homodyne detection is displayed in Fig. 1. To reduce the change of the polarization states and make the whole sensing system reliable and less influenced during the lake test, the fiber in the system is all single-mode polarization fiber. First, a single-mode continuous linear polarization semiconductor laser with the wavelength λ of 1550 nm, the spectral linewidth less than 1 kHz, and the output power of 8 mW is amplified to about 60 mW by an erbium-doped optical fiber amplifier (EDFA). In order to prevent the dangerous backward propagation, there are two polarizing fiber optical isolators following the semiconductor laser and the EDFA. Then this amplified laser is divided into two parts by a 1×2 polarizing fiber optical splitter (PFOS). The first part acts as the local oscillator (LO) laser and the second part serves as the transmitted laser. In order to realize the five-channel detection synchronously, the LO laser and the transmitted laser beam are separated equally into five beams specifically with another two PFOSs. For each transmitted channel, the laser is directed normally and focuses on the water surface after a polarizing fiber optical circulator and a telescope consisting of a single aspherical lens with an aperture of 50 mm and the focal length of 200 mm. Meanwhile, each reflective laser light from the air-water surface is collected by the same telescope and returns to the system participating in the optical beat interference in a single polarizing optical 2×4 90° hybrid with its corresponding LO laser beam. Following, for each channel or each detection point, two balanced photoreceivers (BPs) with a significant capability of suppressing the common noise transfer the mixed optical signal into the electrical signal. The outputs of the BPs are FM signals modulated by the laser Doppler shift frequency produced by the vibration of the water surface. For the five channels detection mode, there are 10 output signals from 10 BPs totally. Correspondingly, a 16-channel DAC with a data sample rate of 10MS/s samples these data. At the same time, the DAC and the function generator to the underwater acoustic transmitter are triggered by the same external trigger unit to ensure the time synchronization of the detection.

As a result of the oscillations of the practical water surface, the signal will be intermittent. Therefore, the signal processing unit is necessary to respond to the coming non-continuous signal information immediately, accurately, and reliably. Considering all of these, for the in-phase signal $i_n(t)$ and quadrature signal

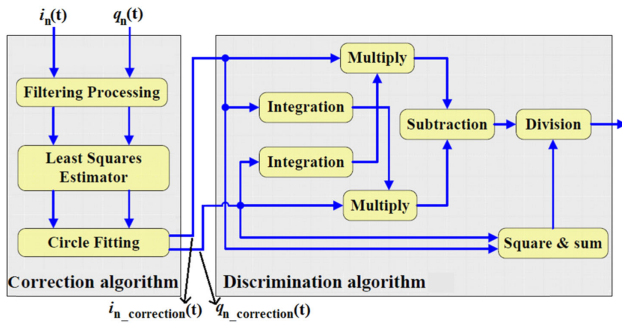


Fig. 2. Signal processing block diagram.

$q_n(t)$ of the n th detection channel, described as Eqs. (1) and (2), the signal processing includes two steps shown in Fig. 2. The first is to undertake the correction algorithm against for the quadrature imbalance and other non-linearity coming from the imbalance between the two beams and imperfect phase bias offset of the optical 90° hybrid. The second is to run the real-time discrimination algorithm for extracting the interested vibration parameters of the water surface:

$$\begin{aligned} i_n(t) &= R\sqrt{P_S \cdot P_{LO}} \cos[2\pi f_d t + (\psi_S - \psi_{LO})] \\ &= I_1 + I_2 \cos[2\pi f_d t + (\psi_S - \psi_{LO})], \end{aligned} \quad (1)$$

$$\begin{aligned} q_n(t) &= R\sqrt{P_S \cdot P_{LO}} \sin[2\pi f_d t + (\psi_S - \psi_{LO}) + \delta] \\ &= Q_1 + Q_2 \cos\left[2\pi f_d t + (\psi_S - \psi_{LO}) + \delta - \frac{\pi}{2}\right], \end{aligned} \quad (2)$$

where R is the ideal BPs' responsivity, P_S and P_{LO} represent the average powers of the returned signal laser and the LO laser at the input of the optical 2×4 90° hybrid, ψ_S and ψ_{LO} describe the phases of them, δ is the phase difference caused by the non-ideal factors, and f_d is the laser Doppler frequency shift introduced by the moving vibration of the water surface, respectively.

Based on the least squares estimator and the algorithm of circle fitting presented in [12,13], the I_1 , I_2 , Q_1 , Q_2 , and δ can be determined using the coefficients obtained from a series of functions. Thus, the set of $i_n(t)$ and $q_n(t)$ collected by each channel of the LDV will fit a unit circle equation consequently. And the original $i_n(t)$ and $q_n(t)$ can be expressed as $i_{n_correction}(t)$ and $q_{n_correction}(t)$, whose phase difference is 90° strictly:

$$i_{n_correction}(t) = \cos[2\pi f_d t + (\psi_S - \psi_{LO})], \quad (3)$$

$$q_{n_correction}(t) = \sin[2\pi f_d t + (\psi_S - \psi_{LO})]. \quad (4)$$

Then, processed with the discrimination algorithm, the final output $u_n(t)$ of the signal processing is shown as Eq. (5). It has a linear relationship with the vibration velocity of the air–water surface $v(t)$:

$$\begin{aligned} u_n(t) &= \frac{\frac{d[q_{n_correction}(t)]}{dt} \cdot [i_{n_correction}(t)] - \frac{d[i_{n_correction}(t)]}{dt} \cdot [q_{n_correction}(t)]}{[i_{n_correction}(t)]^2 + [q_{n_correction}(t)]^2} \\ &= 2\pi f_d = 2\pi \frac{2v(t)}{\lambda}. \end{aligned} \quad (5)$$

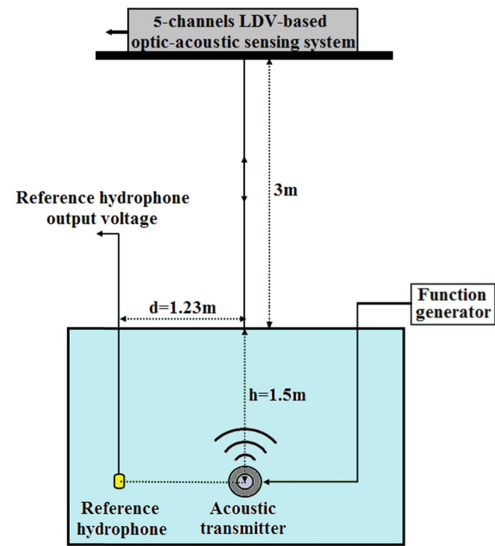


Fig. 3. SPL calibration test setup under the anechoic tank.

3. EXPERIMENTS AND RESULTS

A. Minimum Detectable SPL Calibration Test

The parameters of every channel are the same with each other. Hence, the fifth detection channel is chosen to undertake the calibration testing and demonstrate the system minimum detection capability. The calibration experiment is carried out in the anechoic tank whose length, width, and depth are 8 m, 5 m, and 5 m, respectively. The experiment setup is illustrated in Fig. 3. The five-channel LDV-based acousto-optic sensing system is located on the platform 3 m above the water surface. Since the laser with wavelength of 1550 nm presents a good characteristic of attenuation under water, the underwater acoustic transmitter is submerged to a depth of 1.5 m and just directly below the detection point of the fifth channel. Through a function generator, the underwater acoustic transmitter was set to emit a 2 ms long acoustic pulse of sinusoidal signal with every 0.5 s and the sin frequencies f are 6 kHz, 10 kHz, 20 kHz, 50 kHz, 100 kHz, 150 kHz, and 200 kHz specifically. In order to avoid the disturbance in low frequencies mainly from the surroundings, the tested frequency f starts from 6 kHz. On the other aspect, due to the hydrophone frequency response being limited above 200 kHz, the upper tested frequency is set as 200 kHz.

During the test, the underwater acoustic signal is observed using a traditional, ceramic-based reference hydrophone TC4019 which is horizontally mounted 1.23 m away from the acoustic transmitter. Meanwhile, the fifth channel of the acousto-optic sensing system gives the final demodulated output. Through reducing the amplitude of the function generator, the output of the sensing system will decrease at the same time. And when the detected signal becomes indistinguishable from the background noise, according to the reference hydrophone output voltage U_{OC} and Eq. (6), the minimum detectable SPL and detection SNR of the system can be calculated at this critical point:

$$L_S = 20 \lg(U_{OC} \times d) - M_0 - 20 \lg b, \quad (6)$$

Table 1. SPLs of the LDV-Based Acousto-Optic Sensing System at Different Frequency Bands Under Static Water Surface in the Anechoic Tank

f/kHz	$M_0/\text{dB re V}/\mu\text{Pa}$	$U_{OC}/\mu\text{V}$	$L_S/\text{dB re V}/\mu\text{Pa}$
6	-197.9	22	103.0247
10	-196.6	22	101.7247
20	-196.9	210	121.6207
50	-198.0	280	125.2194
100	-198.8	240	124.6805
150	-198.0	400	128.3175
200	-197.9	500	130.1557

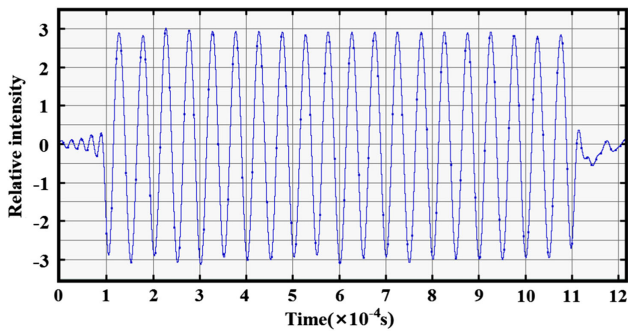


Fig. 4. Time-domain wave format 10 kHz of the system's fifth channel.

where L_S is the acousto-optic sensing system's minimum detectable SPL; U_{OC} is the output voltage of the reference hydrophone TC4019; M_0 is the receive voltage sensitivity of the TC4019 at different tested frequencies ranging from 6 kHz, 10 kHz, 20 kHz, 50 kHz, 100 kHz, 150 kHz, and 200 kHz; $d = 1.23$ m is the horizontal distance between the transmitter and the reference hydrophone; and $h = 1.5$ m is the vertical distance between the underwater acoustic transmitter and the water surface, respectively.

In the case of the hydrostatic surfaces, the corresponding minimum detectable SPLs of this sensing system at the air-water interface at different frequency bands are listed in Table 1. With the short duration signal detection scheme, the system is able to capture the signals with the acoustic pressure as low as 101.73 dB re 1 μPa at 10 kHz, which provides a profound band for the communication between the platform in air and the underwater. And from the corresponding time-domain diagram shown in Fig. 4, it is clear that the sine signal cycle is 0.1 ms and lasts 2 ms totally. Moreover, based on the Fourier transforms of a total of 30 tested records at each frequency band, the SNR sensitivities of the system are still keeping at 22 dB when they reach the level of the minimum detectable SPL. Due to the data sample rate of the DAC of 10 MS/s and the bandwidth of the signal processing, the system presents a wide frequency response range of the Doppler shift and the velocity measurement, which is one essential factor for the acousto-optic application in the practical water situations.

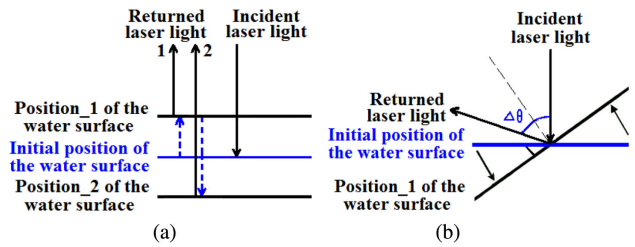


Fig. 5. Water surface movement combined with (a) movement of the ups and downs and (b) movement of the swing.

B. Qiandao Lake Test with Five-Channel LDV-Based Acousto-Optic Sensing System

The laser transmitter and receiver of the designed sensing system are coaxial, and correspondingly require the laser beam incidents the air-water interface nearly perpendicularly. In addition, the laser Doppler frequency shift due to the Doppler effect of the water surface motion is directly proportional to the surface velocity, including the small vibration caused by the underwater sound field and movements caused by the ripples and waves on the water surface. The foremost question of the LDV-based acousto-optic sensing system applied under real environments is how to eliminate the effects resulting from the water motion. To explain the effects more concisely and fundamentally, the water movement model is simplified here. As a fact, the actual movement of the water surface can be described as the complex and random combination of the movement of the ups and downs and the movement of the swing, depicted in Fig. 5.

For the first simplified model, the vibration induced by the underwater sound wave is superimposed on the moving of the water surface from the initial position to the position_1 or position_2. Depending on the vertical moving velocity of the water surface, the data sample rate of the DAC needs to be increased accordingly. Otherwise, the Doppler frequency shift will be lost even if the returned laser light gets back into the receiving field of view totally. Hence, the data acquisition rate of the designed sensing system is 10 MS/s, which can satisfy the requirements under most situations. Related to the movement of the swing, the returned laser light will deviate from the receiving field of view due to the tilt of the water. As the slope angle of the water surface becomes bigger, the signal drop will be much more serious. Figure 6 is the two orthogonal outputs $i_{5_correction}(t)$ and $q_{5_correction}(t)$ of the fifth channel of the sensing system. The fluctuation of the signal carrier-envelope is directly affected by the water moving. When the air-water interface is moving slightly, the time-domain distribution is nearly continuous and the amplitudes of these orthogonal signals are changing with the motion of the reflective point [Fig. 6(a)]. During the period when the water surface is moving significantly, the signal drop is serious and only a limited part of the laser light is able to return to the sensing system, which leads to a large blank area in the time-domain diagram [Fig. 6(b)]. When the original samples are missing, some research related to how to compensate the intermittent signals has been reported. [14,15] However, regarding the continuous signal reconstruction from the irregular non-uniform and similar to a discrete time waveform under hydrodynamic water conditions, it still faces a lot of realistic problems.

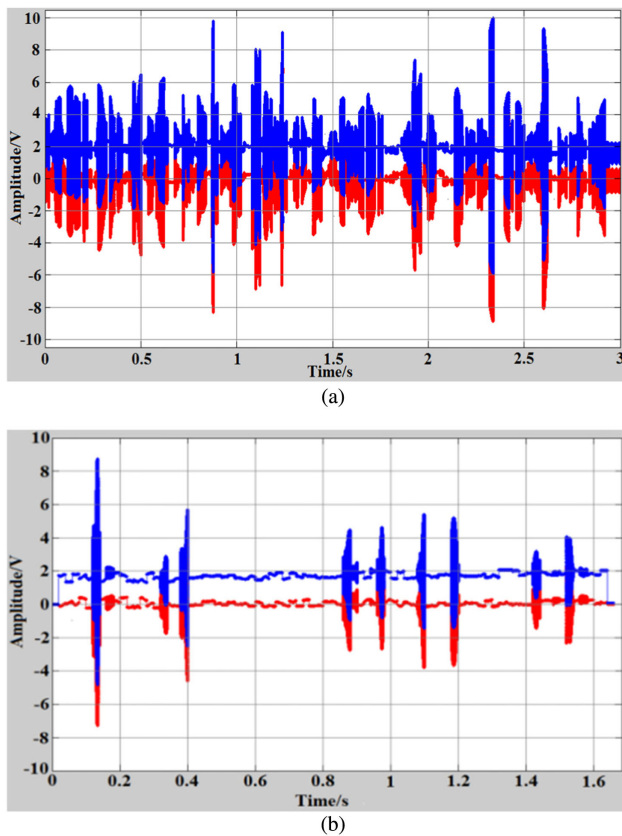


Fig. 6. Output of the fifth channel of the LDV-based acousto-optic sensing system under hydrodynamic water surface.

The signal dropout is the bottleneck why the LDV-based acousto-optic sensing system is limited in the practical application. Thus, there are some solutions answering this question. The first is to increase the receiving field of view of the sensing system. The second is to design the tracking system or the adaptive system to track the movement of the water. The third is to design the scanning LDV or the multi-point LDV to increase the detection probability. Building a large-caliber telescope is an effective means to broaden the receiving field of view and to increase the laser beam diameter. As a fact, considering the difficulty and the manufacturing cycle time of the mirror processing and the contribution to the sensing system, this is not practical or uneconomical in most applications. In addition, the sensing system is implemented according to the principle of the optical coherent detection. The coherence efficiency is critical for its performance. Therefore, for the operated telescope, only by increasing the diameter of the laser beam will contribute to the coherence efficiency decreasing severely. In terms of the second solution, fast steering of the transmitted laser beam by using the galvanometer or motors will introduce an additional Doppler frequency shift component and background noise on the actual vibration information of the air–water interface. Furthermore, the real air–water interface is always moving, either in the lake or others. The amplitude, the frequency, and the alias angle of the water movement are affected by sorts of facets, such as the water flow, water surface state, and air turbulence. As a consequence, the specific motion function describing the exact location where

the sensing system detects the vibration is complex and ambiguous. Realistically, this approach is just an alternative choice to improve the signal dropout rate under the regular moving water surface based on our previous experiments.

In order to eliminate the signal dropout, the multiplexing parallel receiving and compensation for the returned optical signals are applied. When locating the multi-detection channels, it has little to do with the spatial distribution between each channel. The main considering factor is to keep their horizontal distribution against the underwater sound source symmetrical and equidistant. In this way, the receiving angles of the underwater sound wave a kind of spherical wave are almost same. In addition, in view of the characteristic of the water surface slope distribution, the maximum probing probability will be achieved when the optical axis of the telescope is perpendicular to the water surface.

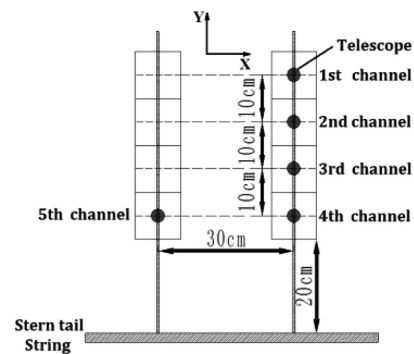


Fig. 7. Top view of the transmitted telescopes arrangement of the five-channel LDV-based acousto-optic remote sensing system.

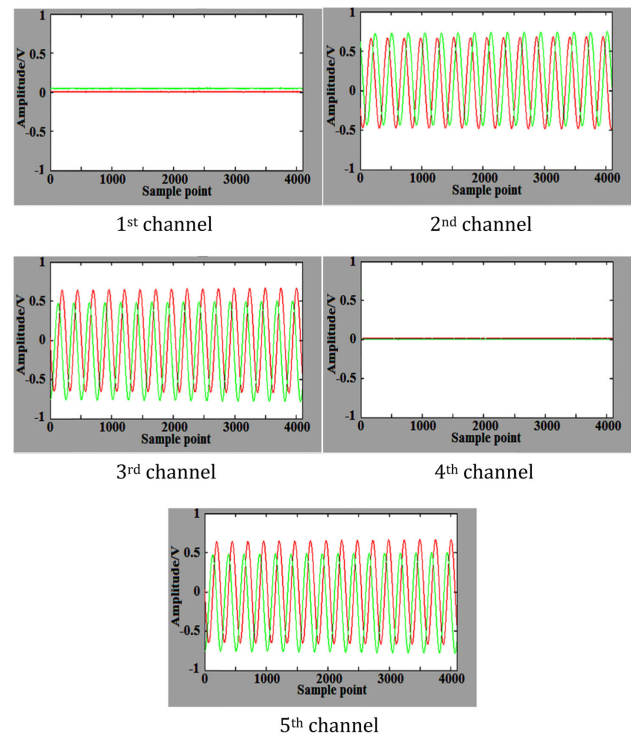


Fig. 8. In-phase and quadrature signals of the five-channel sensing system.

Table 2. Probing Probability of Five Channels Under Hydrodynamic Water Surface in Qiandao Lake

	1st Channel	2nd Channel	3rd Channel	4th Channel	5th Channel
Effective detection points	14951552	30343936	33246080	10396288	58961280
Total detection points	18368×10^4				
Probing probability P_n	8.14%	16.52%	18.10%	5.66%	32.1%

On the basis of these, we prefer the five-channel LDV realizing the acousto-optic sensing array in order to evaluate the performance of the multi-points detection mode versus the realistic water surface. Figure 7 is the arrangement of the five channels of the LDV-based acousto-optic sensing system when the experiment is carried out on a test boat. These five channels are located on two shelves apart from the water surface at 2 m. The first channel to the fourth channel are on the first shelf and the fifth channel is on the second shelf. The distances between the first and fourth channels and between the fourth and fifth channels are 30 cm. The distance between two channels from the first to the fourth channel is 10 cm. And the distance between the telescopes of the fifth channel/fourth channel and the stern tail string is set as 25 cm in order to avoid the blocking from the stern. For each channel, the laser light was focused on the water surface.

In terms of the practical water surface on Qiandao Lake in Zhejiang province in China, the detection sensitivity of the acousto-optic sensing system will decrease with the condition of the water, such as the roughness, amplitude, slope, and spatial frequency of the surface wave motion. Therefore, for the experiments on Qiandao Lake, the main objective is to judge the feasibility of the multi-point detection mode and its improvement to the signal dropout. During the lake experiments, the vibration of the air–water surface located at the other end of the test boat (about 15 m away) was generated by a 1064 nm high-pulse-energy laser whose pulse energy is 6 J, pulse duration is about 8 ns, and repetition rate is 1 Hz. The transmitted laser pulse was set to emit a short pulse laser which gives a challenge to the signal capture of the sensing system under the realistic water surface. In addition, the trigger signals to the DAC of the acousto-optic sensing system and the laser transmitting of the pulsed laser are the same with each other, which guarantees a good consistency in the aspect of the transmitter–receiver synchronization.

Figure 8 is one small segment of real-time record of the five channels of the sensing system conducted in the relative calm water surface of Qiandao Lake. The X axis is the sample point and the Y axis denotes the amplitudes of the orthogonal in-phase and quadrature signals. Taking account into the period of the first 4000 sample points, there is no laser light returned back from the water surface into the first channel and the fourth channel associated with serious signal dropout or a strong motion of water surface. In view of the other channels, the laser beam is able to reflect back to the system and the signals containing the detected acoustic component are fluctuating and changing with the movement of the water surface. Since the natural condition of the air–water surface is random and variable with the time, the signal dropout and the real-time waveforms of the five channels will change synchronously.

Considering the specific experiment situations, whether the detection is effective or not is decided by the background noise on site and the detection sensitivity of the sensing system. Based on the corresponding experimental criteria, the signal probing probability of each single channel is listed in Table 2. The effective probing probability is ranging from 5.66% (fourth channel) to 32.1% (fifth channel). According to Eq. (7), the total probing probability P_{total} of the whole five-channel LDV-based acousto-optic remote sensing system is about 59.77%. Obviously, with the five-channel detection, it is a satisfied result that the signal probing probability is improved from 32.1% to 59.77%. In addition, the synchronization between the five channels of the sensing system and the 1064 nm high-pulse-energy laser through the same clock signal brings the signal compensation into reality:

$$\begin{aligned}
 P_{total} &= 1 - (1 - P_1) \times (1 - P_2) \times (1 - P_3) \times (1 - P_4) \\
 &\quad \times (1 - P_5) = 1 - (1 - 8.14\%) \times (1 - 16.52\%) \\
 &\quad \times (1 - 18.10\%) \times (1 - 5.66\%) \times (1 - 32.1\%) \\
 &= 59.77\%.
 \end{aligned}
 \tag{7}$$

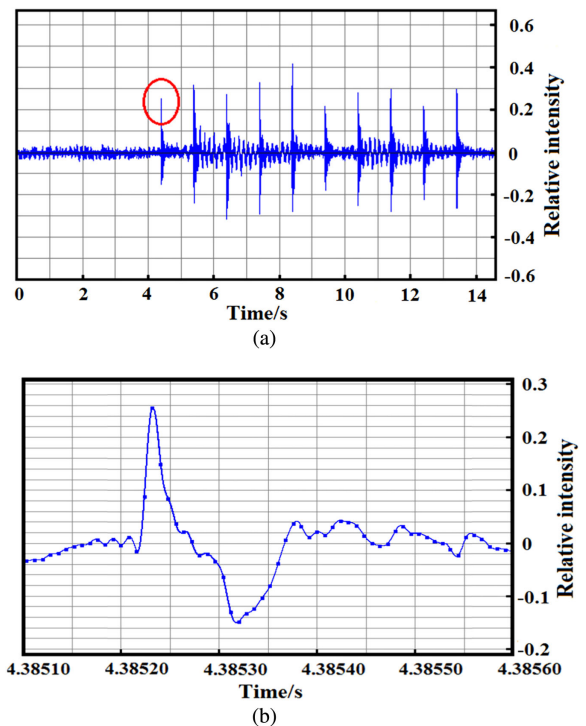


Fig. 9. (a) Recorded time-domain diagram of the acousto-optic system; (b) the details of the recorded time-domain signal between 4.38510 and 4.38560.

Based on the above five channel signals, the final demodulated output of the signal processing is shown in Fig. 9. Figure 9(a) shows the time-domain waveform of the sensing system output. It is the combination of the effective test signals from the five channels on the exact observing time and 10 instances of the tested signal were recorded in total. The frequency of the output signal is 1 Hz and its distribution received a good consistency with the transmitted laser source at the same time. Depending on the oscillations of the hydrodynamic water surface, Fig. 9(a) contains some large amplitude signals when the slope of the water surface is small and many more optical signals return to the system. Figure 9(b) is the expanded time scale of the first pulse signal, which gives the details of the first pulse waveform of the test signal. The pulse duration is nearly equal to that of the transmitted laser pulse of 8 ns.

4. CONCLUSIONS

A high-sensitivity and good signal probing probability all-fiber homodyne five-channel LDV-based acousto-optic sensing system was designed. Under the anechoic tank, the calibration experiments detecting the underwater sound source on the platform 3 m away from the water surface were conducted. This sensing system is capable to acquire the sound pressure and frequency of the underwater sound source by determining the vibration of the water surface. At 10 kHz, the system is able to capture the signals with the acoustic pressure as low as 101.73 dB/ μ Pa. These minimum detectable SPLs and the wide frequency response range are great improvements for the practical application. For the hydrodynamic water surface condition, the reason for the signal dropout is analyzed and some alternative approaches are discussed. Based on the multiplexing parallel receiving and compensation of the returned signals, the five-channel LDV-based sensing system is applied to capture the vibration of the air–water interface generated by a high-power short-duration pulsed laser. With the test on Qiandao Lake, for the relative calm water condition, the probing probability P_{total} of the whole sensing system is 59.77% higher than that of the single channel (32.1%). It proved that multi-detection channels can eliminate the signal dropout. Furthermore, with more channels, the P_{total} will be much better. For these reasons, it is one promising direction to detect the underwater sound or communicate with the underwater platform.

Funding. National Natural Science Foundation of China (51403034); State Key Laboratory for Modification of Chemical Fibers and Polymer Materials (LK1113).

Acknowledgment. The authors acknowledge researchers from the Zhejiang University and the National Defence Underwater Acoustics Calibration Laboratory for their

technical assistance with the calibration test facility and experimentation. Thanks for the support of “Open Fund of Shanghai Center for High Performance Fibers and Composites.”

Disclosures. The authors declare no conflicts of interest.

REFERENCES

1. A. R. Harland, J. N. Petzing, and J. R. Tyrer, “Nonperturbing measurements of spatially distributed underwater acoustic fields using a scanning laser Doppler vibrometer,” *J. Acoust. Soc. Am.* **115**, 187–195 (2004).
2. L. T. Antonelli and F. A. Blackmon, “Experimental demonstration of remote, passive acousto-optic sensing,” *J. Acoust. Soc. Am.* **116**, 3393–3403 (2004).
3. D. Farrant, J. Burke, L. Dickinson, P. Fairman, and J. Wendoloski, “Opto-acoustic underwater remote sensing (OAUROS)—an optical sonar?” in *Proceedings of the IEEE Oceans*, Sydney, NSW, Australia, 2010, pp. 1–7.
4. F. A. Blackmon and L. T. Antonelli, “Experimental detection and reception performance for uplink underwater acoustic communication using a remote, in-air, acousto-optic sensor,” *IEEE J. Ocean. Eng.* **31**, 179–187 (2006).
5. P. O’Malley, J. Vignola, and J. Judge, “Generalized laser Doppler vibrometer noise maps,” *AIP Conf. Proc.* **1457**, 24–34 (2012).
6. P. Land, D. Robinson, J. Roeder, D. Cook, and A. K. Majumdar, “Integration of a laser Doppler vibrometer and adaptive optics system for acoustic-optical detection in the presence of random water wave distortions,” *Proc. SPIE* **9827**, 982702 (2016).
7. B. A. Cray, S. E. Forsythe, A. J. Hull, and L. E. Estes, “A scanning laser Doppler vibrometer acoustic array,” *J. Acoust. Soc. Am.* **120**, 164–170 (2006).
8. K. Maru and K. Watanabe, “Non-mechanical scanning laser Doppler velocimetry with sensitivity to direction of transverse velocity component using optical serrodyne frequency shifting,” *Opt. Commun.* **319**, 80–84 (2014).
9. C. Yang, M. Guo, H. Liu, K. Yan, and Y. Fu, “A multi-point laser Doppler vibrometer with fiber-based configuration,” *Rev. Sci. Instrum.* **84**, 121702 (2013).
10. X. D. Peng, W. Xu, X. F. Jin, and J. H. Shang, “Adaptive filter design for suppressing the moving surface interferences in optic-acoustic remote sensing,” in *Proceedings of IEEE Oceans*, San Diego, California, USA, 2013, pp. 1–6.
11. F. Tonolini and F. Adib, “Networking across boundaries: enabling wireless communication through the water-air interface,” in *Proceeding of the 2018 Conference of the ACM Special Interest Group on Data Communication* (2018), pp. 117–131.
12. W. G. He, B. T. Wang, and C. P. Yang, “Noisy Doppler signal processing for homodyne laser vibrometer system,” *J. Optoelectron. Laser* **22**, 1842–1846 (2011).
13. C. M. Wu, C. S. Su, and G. S. Peng, “Correction of nonlinearity in one-frequency optical interferometry,” *Meas. Sci. Technol.* **7**, 520–524 (1996).
14. A. Zaeemzadeh, M. Joneidi, and N. Rahnavard, “Adaptive non-uniform compressive sampling for time-varying signals,” arXiv170303340 (2017).
15. H. Johansson and P. Löwenborg, “Reconstruction of nonuniformly sampled bandlimited signals by means of time-varying discrete-time FIR filters,” *EURASIP J. Adv. Signal Process.* **2006**, 064185 (2006).